RESEARCH ARTICLE

Propolis from the Stingless Bee *Trigona incisa* from East Kalimantan, Indonesia, Induces *In Vitro* Cytotoxicity and Apoptosis in Cancer Cell lines

Paula M Kustiawan[1,5], Preecha Phuwapraisirisan[2], Songchan Puthong[3], Tanapat Palaga[4], Enos T Arung[5], Chanpen Chanchao[6]*

Abstract

Background: Previously, stingless bee (*Trigona* spp.) products from East Kalimantan, Indonesia, were successfully screened for *in vitro* antiproliferative activity against human cancer derived cell lines. It was established that propolis from *T. incisa* presented the highest *in vitro* cytotoxicity against the SW620 colon cancer cell line (6% cell survival in 20 μg/mL). Materials and Methods: Propolis from *T. incisa* was extracted with methanol and further partitioned with n-hexane, ethyl acetate and methanol. The *in vitro* cytotoxicity of the extracts was assessed by the MTT assay against human colon (SW620), liver (Hep-G2), gastric (KATO-III), lung (Chago) and breast (BT474) cancer derived cell lines. The active fractions were further enriched by silica gel quick column, absorption and size exclusion chromatography. The purity of each fraction was checked by thin layer chromatography. Cytotoxicity in BT-474 cells induced by cardanol compared to doxorubicin were evaluated by MTT assay, induction of cell cycle arrest and cell death by flow cytometric analysis of propidium iodide and annexin-V stained cells. Results: A cardol isomer was found to be the major compound in one active fraction (F45) of T. incisa propolis, with a cytotoxicity against the SW620 (IC_{50} of 4.51 ± 0.76 μg/mL), KATO-III (IC50 of 6.06 ± 0.39 μg/mL), Hep-G2 (IC_{50} of 0.71 ± 0.22 μg/mL), Chago I (IC_{50} of 0.81 ± 0.18 μg/mL) and BT474 (IC50 of 4.28 ± 0.14 μg/mL) cell lines. Early apoptosis (programmed cell death) of SW620 cells was induced by the cardol containing F45 fraction at the IC_{50} and IC_{80} concentrations, respectively, within 2-6 h of incubation. In addition, the F45 fraction induced cell cycle arrest at the G1 subphase. Conclusions: Indonesian stingless bee (*T. incisa*) propolis had moderately potent *in vitro* anticancer activity on human cancer derived cell lines. Cardol or 5-pentadecyl resorcinol was identified as a major active compound and induced apoptosis in SW620 cells in an early period (≤ 6 h) and cell cycle arrest at the G1 subphase. Thus, cardol is a potential candidate for cancer chemotherapy.

Keywords: *Trigona incisa* - propolis - cardol - apoptosis - cell arrest

Asian Pac J Cancer Prev, **16 (15)**, 6581-6589

Introduction

Both genetic and environmental factors are known to play a role in causing cancer (Iwasaki and Tsugane, 2011). For the last few decades the standard cancer treatments have involved surgery, radiation and chemotherapy. However, metastatic disease frequently redevelops even after surgery. In addition, the typical systemic treatment regime has often led to intolerable side-effects. Chemotherapeutic drugs still have a lot of constrained problems, including not being selective in killing cancer cells but also inducing normal cell death. Although the mode of action of these drugs is to affect the synthesis of nucleic acids and/or proteins, drug resistant cancers have been found. For example, rhabdomyosarcoma was reported to be resistant to platinum-based chemotherapy, where neurotoxicity is the main dose-limiting side effect that prevents higher systemic doses being administered (Donzelli et al., 2004; Jeong et al., 2014). In addition, the extremely rare metastatic spermatocytic seminoma with sarcomatous transformation has been reported to be highly resistant to cytotoxic chemotherapy (Wetherell et al., 2013). Many alternative chemotherapeutic agents have been discovered, such as osthole, one of the coumarins isolated from Prangos ferulacea (L.) that is a potential therapeutic cytotoxic agent, especially against the human prostate cancer cell line (PC3) (Shokoohinia et al., 2014), and lupeol, a dietary triterpene isolated from many fruits and medicinal plants that has shown an anti-cancer effect on the gallbladder carcinoma cell line (GBC-SD) (Liu et al., 2014). However, the side effects induced by these compounds and the costs of treatment with them were

*Department of Biology, Faculty of Science, Chulalongkorn University, Bangkok, Thailand *For correspondence: chanpen@sc.chula.ac.th*

both quite high. This has led to an increased interest to try alternative treatments including those that use "*natural*" ingredients (Stetler-Stevenson, 2001).

Moreover, synergistic and additive combinations of compounds are of increasing interest as treatment agents in cancer treatment. For example, the combination of the subfraction of Strobilanthes crispus leaves and tamoxifen, an anti-estrogen drug, showed a strong *in vitro* synergistic inhibition of the breast cancer cell lines MCF-7 and MDA-MB-231, but appeared non-cytotoxic at these doses to the non-malignant MCF-10A cell line (Yaacob et al., 2014).

In recent years, bee products and especially propolis have become a point of particular interest because they have been shown to exhibit a broad spectrum of bioactivities (Bankova and Popova, 2007). Normally, bees make propolis for a diverse array of uses, including for nest construction, chemical defense and honey preservation from microbial spoilage (Boorn et al., 2010).

Many compounds have been isolated from different propolis sources (geographical locations and originating bee species). Most of them belong to phenolic acids and their esters, flavonoids (flavones, flavanones, flavonols, dihydroflavonols and chalcones), terpenes, aromatic aldehydes and alcohols, fatty acids, stilbenes and steroids (Burdock, 1998). However, the most researched component of propolis is caffeic acid phenethyl ester, which exhibits antiproliferative, anti-inflammatory, antineoplastic, antimicrobial and antioxidative activities (Burdock, 1998).

Other interesting examples of bioactive compounds in propolis include the C-methyl flavanones in the propolis from the stingless bee Tetragonula carbonaria in Australia (Massaro et al., 2014). The bees harvested these compounds from the fruit resin of Corymbia torelliana. These C-methyl flavanones could inhibit Staphylococcus aureus ATCC 25923 much better than Pseudomonas aeruginosa ATCC 27853 and were accepted as chemomarkers in both mentioned propolis and fruits of C. torelliana (Massaro et al., 2014).

The geopropolis (a mixture of resin, wax and soil) from the stingless bee Melipona scutellaris from the northeast region of Brazil decreases the production level of IL-1β and TNF-α (Franchin et al., 2012). As key parameters in inflammation responses, this suggests an anti-inflammatory role.

Since bees harvest the key components from plants, differences in the native plants of each country or region, or in the foraging strategy of different bee species/isolates could directly affect the chemical compounds and their bioactivities. With this in mind, we continued the work reported by Kustiawan et al. (2014). In this study here, this same propolis was further fractionated in order to ascertain the main active compound(s), and their potential mode of action including the induction of apoptosis (programmed cell death) and cell cycle arrest.

Materials and Methods

Sample collection

Trigona incisa propolis was collected from Mulawarman University Botanical Garden, Samarinda, Indonesia, in February of 2013. The raw propolis was cleared of residual bees and bee larvae and then wrapped with aluminum foil (light protection) and kept at -20°C until use.

Partition

Propolis (500 g) was cut into small pieces and extracted in 800 mL of 96% (v/v) methanol (MeOH) at room temperature (RT) with continuous shaking (7400 Tübingen; Edmun Buchler, Germany) at 100 rpm for 24 h. The suspension was filtered through Whatman filter paper No. 2 (Sigma-Aldrich, Germany) and the solvent was removed from the filtrate by evaporation at 40°C in a vacuum oven to near dryness to yield the initial MeOH extract. The solid residue (extracted propolis) was extracted in the same manner until the color of the extract was almost clear (three more extractions) and the obtained crude extracts were pooled. A portion of the pooled crude extract was then dissolved in 60% (v/v) aqueous MeOH, volume as required for complete solvation. It was partitioned at RT with an equal volume of n-hexane and then left for 24 h for phase separation. The two phases were kept separate. The upper n-hexane phase was evaporated as above to leave the crude hexane extract (CHE), whilst the lower MeOH phase was further partitioned at RT with an equal volume of ethyl acetate (EtOAc), and then left for phase separation and saved. The EtOAc in the upper phase was removed by evaporation as above to yield the crude EtOAc extract (CEE), whilst the lower phase yielded the crude MeOH extract (CME) after solvent removal. Each crude extract was weighed, its character recorded, and then stored wrapped in aluminum foil at -20°C until use.

Enrichment and fractionation of components by column chromatography (CC)

Silica gel quick CC: The silica gel CC was prepared by adding silica gel 60 G (0.063-0.2 mm) into a sintered glass (250 mL) and tightly packing the silica gel under a vacuum. Each crude extract was mixed with silica gel 60 until it was not sticky and then loaded onto the top of the packed silica. A piece of filter paper (Whatman, qualitative circle of 110 mm in θ) was laid on top of the packed silica. The column was eluted with a discontinuous sequential (1.5 L of each) 0:1, 1:3, 1:1, 3:1 and 1:0 (v/v) dichloromethane (CH_2Cl_2): hexane and 1:24 and 3:7 (v/v) MeOH: CH_2Cl_2 gradient and collecting 75 mL fractions. The chemical profile of each fraction was checked by one dimensional thin layer chromatography (1D-TLC), as detailed in section 2.3.4. Fractions with a similar 1D-TLC profile were pooled together. For all fractions or pooled fractions the solvent was then evaporated at 40 oC under vacuum. The residual fraction was weighed, characterized and screened for antiproliferative activity against the human cancer derived cell lines (section 2.5.2).

Absorption CC: Each fraction from the silica gel quick CC (section 2.3.1) that showed any cytotoxic activity was further fractionated by absorption CC. The column (250 mL in volume) was packed with silica gel 60 prequilibrated in hexane (200 mL) to the proper height. The respective sample was mixed with silica gel 60 (5-7g) at RT and left until dry, when it was then laid on top of the column.

The residual hexane solvent was removed in order that the sample was better absorbed into the silica gel, whilst additional silica gel was placed on top of the column so that the layer containing the sample was smooth. Finally, a layer of cotton was laid on top and the left over solvent was removed. The column was eluted with 500 mL of each (sequentially) of a 0:1, 2:3 and 3:2 (v/v) EtOAc: hexane and 100% (v/v) MeOH. All eluted fractions (2.5 mL/ fraction) were collected and the chemical profile of each fraction was determined by 1D-TLC as per section 2.3.4. Fractions with a similar 1D-TLC pattern were pooled and then the solvent from all the fractions or pooled fractions was evaporated in rotary evaporator (40°C) under vacuum and the residue was screened for *in vitro* cytotoxic activity against the cell lines (section 2.5).

Size exclusion CC: Further fractionation and enrichment of the active fractions from the absorption chromatography was performed by size exclusion CC using a Sephadex LH-20 column (250 mL internal volume). Each respective fraction was dissolved in a 1:4 (v/v) ratio of EtOAc: n-hexane until it was not sticky and was loaded on top of the column. The column was then eluted with 250 mL of a 1:4 (v/v) ratio of EtOAc: n-hexane collecting 2 mL fractions. The fractions were then evaporated in rotary evaporator (40°C) under vacuum, the residue weighed, visually characterized and an aliquot checked by 1D-TLC. In addition, each fraction was checked for cytotoxic activity (section 2.5).

Sample analysis by 1D-TLC: The 1D-TLC plate was comprised of percolated Merck Kieselgel 60 F254 and RP-18 F254 plates (0.25 or 0.50 mm thickness), respectively, and was cut to a 5 x 5 cm size. An aliquot of each fraction (diluted by soluble organic solvent if it was too sticky) was spotted (~2 μL) onto five TLC plates at 0.5 cm above the bottom of each TLC plate using a capillary tube. Loaded TLC plates were then air dried, placed into the TLC chamber and resolved to a solvent front within 0.5 cm of the top of the plate using a mobile phase of (i) 100% (v/v) n-hexane, (ii) 6:4 (v/v) ratio of n-hexane: EtOAc, (iii) 100% (v/v) CH_2Cl_2, and (iv) 1:49 (v/v) MeOH: EtOAc. Each TLC plate was then left at RT until dry and the location of the compounds were visualized under ultraviolet light (λ = 256-380 nm).

Structure identification: Nuclear magnetic resonance (NMR) spectra were measured on a Bruker Advance 400 MHz NMR spectrometer with tetramethylsilane (TMS) as the internal standard and deuterated chloroform (CDCl3) as the solvent. Furthermore, an evaporated purified fraction 45 (1-2 mg) was dissolved in ethyl acetate (1 ml) and sent to National Science and Technology Development Agency (NSTDA) for the service to search for molecular weight. Electrospray ionization mass spectroscopy (ESIM) was a selected mode used to run MS.

Cytotoxicity

Cell culture: The human cancer derived cell lines used in this study were derived from ductal carcinoma (BT474, ATCC No. HTB20), lung undifferentiated cancer (Chago I, National Cancer Institute, Thailand), liver hepatoblastoma (Hep-G2, ATCC No. HB8065), gastric carcinoma (KATO-III, ATCC No. HTB103) and colon adenocarcinoma (SW620, ATCC No. CCL227). In addition, the normal skin fibroblast cell line (CCD-986sk, ATCC No. CRL1947) was used for comparison. All cell lines were obtained from the Institute of Biotechnology and Genetic Engineering, Chulalongkorn University, and were used at passage number 115 for BT474, 286 for Chago I, 57 for Hep-G2, 134 for KATO-III, 160 for SW620 and CCD-986sk. Cell lines were cultured in complete medium (CM: RPMI 1640 medium containing 5% (v/v) fetal calf serum) at 37°C supplied with 5% (v/v) CO_2, seeding at 10^5 cells/25 cm^2 flask in 5 mL CM, and repassaging when at 70-80% confluency, except DMEM (Dulbecco's modification of Eagle's medium) was used in place of RPMI for CCD-986SK.

Cytotoxicity assay using [3-(4,5-dimethyl-thiazol-2-yl)2,5-diphenyl-tetrazolium bromide] (MTT)

The potential cytotoxicity (anti-proliferative and/or reduced cell viability) of each fraction was assayed using the surrogate cell viability (MTT) assay. In brief, cultured cells (5,000 cells) in 198 µL of CM were transferred into each well of a flat 96 well plate and then incubated at 37°C in a humidified air atmosphere enriched with 5% (v/v) CO_2 for 24 h in order to let the cells attach to the bottom of each well. Test samples were serially diluted in dimethyl sulfoxide (DMSO) and then for each dilution 2 μL was added to triplicate wells. The addition of DMSO only was performed as the solvent control. Cells were then cultured for 48 h prior to the addition of 10 µL of a 5 mg/ mL of MTT solution into each well and cultured for 4 h. The media was then removed and a mixture of DMSO (150 µL) and 0.1 mol/L glycine (25 µL) was then added to each well and mixed to lyse the cells and dissolve the formazan crystals. The absorbance was then measured at 540 nm (A540) on a microplate reader. Three replications of each experiment were performed. The number of viable cells, as a % of that in the control group, was then assumed from the A540 ratio of the respective test sample to that of the control, taking the control to be 100% viability. Thus, the assay approximated the sum of any differential proliferation and cell viability, and is referred to herein as the cytotoxicity without discrimination of the two activities.

$$\% \text{ cell survival} = [(At-Ab)/ (Ac-Ab)] \times 100$$

where At, Ab and Ac are the absorbance values of the test sample, blank and control (DMSO addition only), respectively. The concentration to cause a half maximal inhibition (IC_{50}),or that for 20% or 80% maximal inhibition (IC_{20} and IC_{80}) was derived from the equation of the best fit line to the plot of cell survival (%) against fraction concentration.

Data analysis

Data are presented as the mean ± one standard deviation (1SD), and were derived from the indicated number of independent repeats.

Apoptosis (programmed cell death) assay

The induction of apoptosis by the selected enriched

fractions was screened for using the SW620 cell line. Six groups of cells (10^8 cells/mL) were prepared as: (i and ii) untreated cells (controls), (iii-v) cells treated with the selected fraction at the IC_{80}, IC_{50} and IC_{20} concentration, which for fraction F45 was 6, 4.51 and 1.01 μg/mL, respectively, and (vi) doxorubicin-treated cells (0.5 μg/mL) as a positive control. Cells were treated for 2, 4 and 6 h, harvested by centrifugation (670x g, 4 °C for 5 min), washed 1 mL of cold phosphate buffered saline pH 7.2 (PBS: 137 mM NaCl, 2.7 mM KCl, 10.6 mM Na2HPO4 and 0.7 mM KH_2PO_4) and harvested by centrifugation as above, and then resuspended in 50 μL of 1x binding buffer pH 7.4 (10 mM Hepes, 140 mM NaCl and 2.5 mM $CaCl_2$). The cells were then stained, except for the unstained control group (i), by the addition of 1 μL of annexin V (Alexa Fluor 488 conjugate, cat. # A13201, Life Technologies) and 5 μL of 1 mg/mL propidium iodide (PI) solution (P4864, Sigma Aldrich) and incubating at RT in the dark for 30 min, prior to flow cytometric analysis at an emission wavelength of 488 nm using a FC 500 MPL cytometer (Beckman Coulter). Experiments were performed in duplicate.

Cell arrest assay

Five groups of SW620 cells (1 x 10^6 - 1 x 10^8 cells/mL for each group) were prepared as (i) untreated cells (control), (ii-iv) cells treated with the selected fraction (F45) at the IC_{80}, IC_{50} and 3 x IC_{50} concentration and (v) cells treated with doxorubicin at 0.5 μg/mL (positive control). After cells had been treated for 6 h, they were washed with 1 mL cold PBS, harvested by centrifugation (2,000x g, RT for 5 min and fixed by resuspension in 500 μL of cold PBS/200 μL of 70% (v/v) EtOH at -20°C overnight or on ice for 4 h. The cells were then harvested and washed as above, resuspended in 250 μL of PBS and incubated with RNase (0.1 mg/mL) at 37°C for 30 min prior to harvesting as above and resuspending in 12.5 μL of 1 mg/mL PI at RT in the dark for 30 min. The cells were then analyzed by flow cytometry. Experiments were performed in duplicate.

Results

The propolis obtained from Trigona incisa at this site was brown and sticky in appearance. Interestingly, the propolis pot was large in size (Figure 1).

From the initial 500 g propolis, 100 g of CME was obtained and its subsequent sequential partitioning by the three organic solvents resulted in the highest yield of CEE, followed by CME and CHE (Table 1).

The crude extracts were then screened for *in vitro* cytotoxic activity against the five human cancer derived cell lines, plus the normal skin fibroblast (CCD-98sk) cell line for comparison. The derived IC_{50} value was calculated. Only the CEE was found to exhibit any reasonable cytotoxic activity (i.e. a derived IC_{50} value of < 10 μg/mL), with an IC_{50} of 8-9 μg/mL against four of the five cancer cell lines (Table 2). Interestingly, the CEE was less cytotoxic to the normal cell line (CCD-98sk). Accordingly, the CEE fraction was further fractionated.

Silica gel quick CC separation of a 20 g portion of the CEE using an n-hexane/EtOAc gradient as the mobile phase yielded 20 fractions (F1-20). However, four sets of

Figure 1. Trigona incisa hive in a tree trunk in Mulawarman University Botanical Garden, Samarinda, Indonesia. Honey pot and propolis are visible

Table 2. Cytotoxic Activity (as the IC_{50} (μg/mL) Value) of the Crude Partitioned Propolis Extracts

Cancer cell line	IC_{50} (μg/mL)		
	CME	CHE	CEE
BT474	> 10	> 10	> 10
Hep-G2	> 10	> 10	8.94 ± 1.02
Chago I	> 10	> 10	8.26 ± 0.08
SW620	> 10	> 10	8.65 ± 0.06
KATO-III	> 10	> 10	8.06± 0.08
CCD-98sk	> 10	> 10	> 10

*Data are shown as the mean ± 1SD, derived from three repeats

Table 1. Character and Yield of the Obtained Crude Propolis Extracts

Crude extract	Character	Weight (g)	Yield[1] (%)	Yield[2] (%)
CHE	Light yellow and sticky liquid	15.2	15.2	3.04
CEE	Red brown and sticky solid	51.9	51.9	10.4
CME	Dark brown into black solid	28.9	28.9	5.78

Yield as the weight % of the [1]CME and [2]propolis

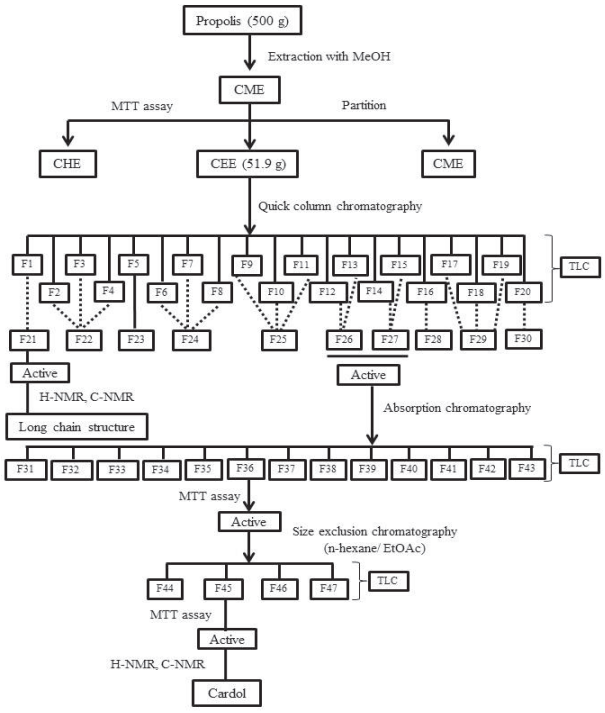

Figure 2. Bioassay guided fractionation of the propolis

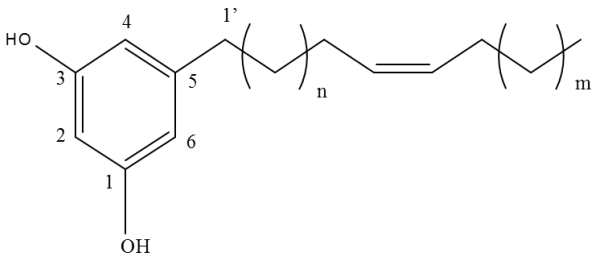

Figure 3. Chemical structure of the active compound in fraction F45. Fraction 45: orange solid; DT46-3; 1H NMR (CDCl3, 400 MHz) δH 6.17 (2H, d, J = 2.0 Hz, H-4, and H-6), 6.10 (1H, s, H-2), 5.28 (2H, m, olefinic proton), 2.39 (2H, t, J = 7.6 Hz, H-1'), 1.95 (4H, br s), 1.48 (2H, br s), 1.18-1.25 (38H, br s), 0.82 (3H, t, J = 6.8 Hz); 13C NMR (CDCl3, 100 MHz) δC 156.5, 146.2, 129.9, 129.8, 108.0, 100.1, 35.8, 31.9, 31.1, 29.8, 29.7, 29.7, 29.6, 29.5, 29.5, 29.3, 27.2, 26.9, 22.3, 14.0; ESIMS m/z [M+H]+ 459 corresponding to molecular formula of $C_{31}H_{54}O_2$

three fractions and two pairs of fractions showed similar TLC profiles and so were pooled, giving ten fractions (F21-30) with unique TLC profiles (Figure 2), which were then screened for *in vitro* cytotoxic activity (Table 3). The BT474 cell line showed no effective growth inhibition (IC_{50}>10 μg/mL) to all 10 fractions, but with respect to the other four cell lines, fraction F26 was cytotoxic to all four of the cell lines (IC_{50} of 5.1-7.8 μg/mL), while F21 and F27 were moderately to weakly cytotoxic to SW620 and Hep-G2. Fraction F24 was only weakly cytotoxic (IC_{50} of 8.2 and 9.4 μg/mL) to two of these cell lines and so was not evaluated any further.

Since fraction F21 showed only one band on the TLC plate, it was analyzed for its chemical structure. The

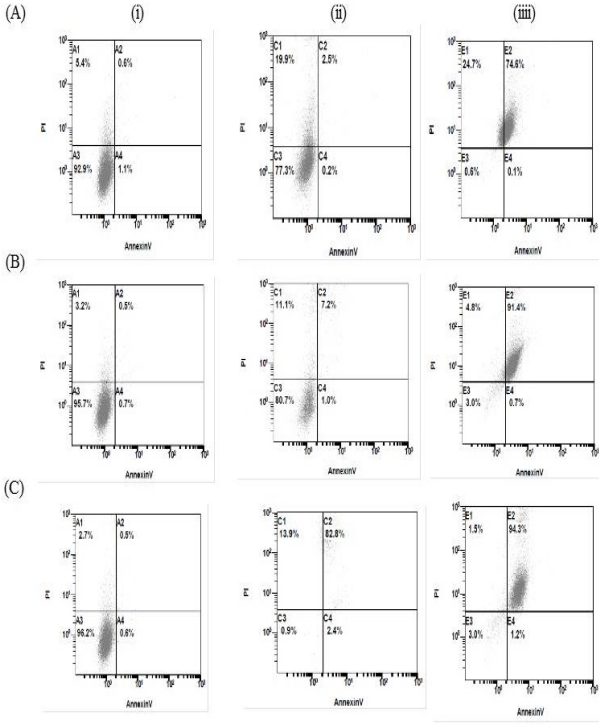

Figure 4. Flow cytometric Analysis of SW620 Cells Stained for annexin-V and PI after incubation of cells in (i) CM only, (ii) F45 at the IC_{80} and (iii) doxorubicin at 0.5 μg/mL for (A) 24 h, (B) 48 h and (C) 72 h. FACS profiles shown are for 2 events and are representative of those seen from two replications

Table 3. Cytotoxicity (as the IC_{50} value) of the F21-30 Fractions Obtained by Quick Column Chromatography

Fraction	Weight (g)	Yield (%)	IC_{50} (μg/mL)					Character
			Chago I	SW620	KATO-III	Hep-G_2	BT474	
F21	0.1	0.5	5.17 ± 1.76	7.76 ± 0.57	> 10	8.93 ± 1.96	> 10	White oily
F22	1.4	7	> 10	> 10	> 10	> 10	> 10	Sticky bright yellow
F23	3.1	15.5	> 10	> 10	> 10	> 10	> 10	Sticky dark yellow
F24	2.6	13	> 10	> 10	9.35 ± 0	8.21 ± 0	> 10	Sticky orange
F25	2.7	13.5	> 10	> 10	> 10	> 10	> 10	Sticky dark orange
F26	2.4	12	5.93 ± 0.36	7.76 ± 0.28	6.75 ± 1.15	5.17 ± 1.36	> 10	Sticky orange brownish
F27	0.7	3.5	> 10	8.08 ± 0.18	6.61 ± 1.29	7.28 ± 0.88	> 10	Sticky red brownish
F28	0.6	3	> 10	> 10	> 10	> 10	> 10	Sticky brown
F29	1.9	9.5	> 10	> 10	> 10	> 10	> 10	Brown solid
F30	3.2	16	> 10	> 10	> 10	> 10	> 10	Black solid

Data are shown as the mean ± 1SD, derived from three repeats

Table 4. Cytotoxicity (as the IC_{50} value) of the F21-30 Fractions Obtained by Quick Column Chromatography

Fraction	Weight (g)	Yield (%)	IC_{50} (μg/mL)					Character
			Chago I	SW620	KATO-III	Hep-G_2	BT474	
F31	0.02	0.67	> 10	> 10	> 10	> 10	> 10	White oily
F32	0.06	2	> 10	> 10	> 10	> 10	> 10	Sticky bright yellow
F33	0.11	3.67	> 10	> 10	> 10	> 10	> 10	Sticky yellow
F34	0.04	1.33	> 10	> 10	> 10	> 10	> 10	Sticky bright orange
F35	0.1	3.33	> 10	> 10	> 10	> 10	> 10	Sticky orange
F36	0.08	2.67	6.34 ± 0.18	7.21 ± 0.20	9.75 ± 0.19	5.55 ± 0.19	7.55 ± 0.24	Sticky dark orange
F37	0.03	1	> 10	> 10	> 10	> 10	> 10	Sticky dark red
F38	0.07	2.3	> 10	> 10	> 10	> 10	> 10	Sticky dark red
F39	0.03	1	> 10	> 10	> 10	> 10	> 10	Sticky red brownish
F40	0.05	1.67	> 10	> 10	> 10	> 10	> 10	Sticky orange brown
F41	0.08	2.67	> 10	> 10	> 10	> 10	> 10	Brown solid
F42	0.33	11	> 10	> 10	> 10	> 10	> 10	Dark brown solid
F43	1.17	39	> 10	> 10	> 10	> 10	> 10	Black brownish solid

Data are shown as the mean ± 1 SD, derived from three repeats

Table 5. Cytotoxic Activity (as the IC_{50} Value) of the Fractions (F44-47) Obtained from Size Exclusion Chromatography of F36

Fraction	Weight (g)	Yield (%)	IC_{50} (μg/mL)						Character
			Chago I	SW620	KATO-III	Hep-G_2	BT474	CCD-986sk	
F44	12	15	> 10	> 10	> 10	> 10	> 10	> 10	Bright yellow
F45	25	31.25	0.81 ± 0.18	4.51 ± 0.76	6.06 ± 0.39	0.71 ± 0.22	4.28 ± 0.14	7.88 ± 0.19	Orange solid
F46	19	23.75	4.55 ± 0.23	6.77 ± 0.19	8.25 ± 0.22	> 10	8.67 ± 0.18	5.24 ± 0.37	Pink solid
F47	38	47.5	> 10	> 10	> 10	> 10	> 10	> 10	Yellow
Doxorubicin			0.45 ± 0.28	0.43 ± 1.32	0.33 ± 0.21	0.31 ± 0.19	0.71 ± 0.22	0.79 ± 0.17	

Data are shown as the mean ± 1 SD, derived from three repeats

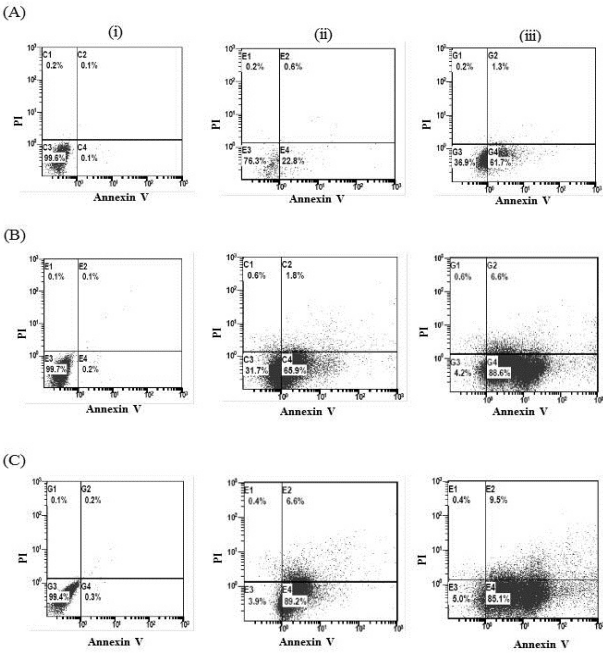

Figure 5. Flow Cytometric Analysis of SW620 Cells Stained for Annexin-V and PI After Incubation of Cells in (i) CM Only and (ii, iii) F45 at (ii) the IC_{50} and (iii) the IC_{80} for (A) 2 h, (B) 4 h and (C) 6 h. FACS Profiles Shown are for 2 Events and are Representative of those seen from two Replications

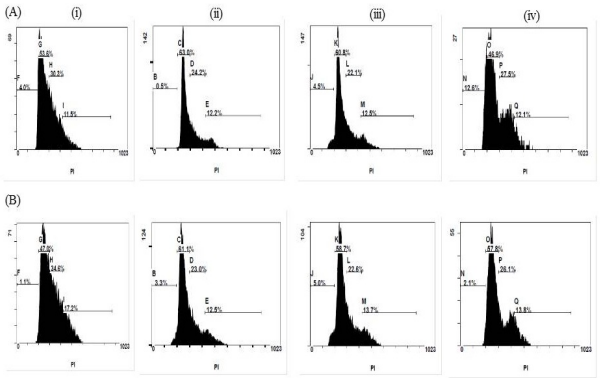

Figure 6. Cell cycle arrest of SW620 cells after treatment for 6 h with (i) CM only, F45 at (ii) 2 x IC_{50} and (iii) 3 x IC_{50} and (iv) doxorubicin at 0.5 μg/mL. Histograms (2 events) shown are representative of those seen from two replications (A and B)

structure was not fully resolved because too small amount (0.1 g or 0.5 % yield) was obtained. However, it was deduced to be a long chain fatty acid structure. Fractions F26 and F27 had same major spot in their respective TLC patterns and so they were pooled together (total weight of 3 g) and further fractionated by absorption CC. After elution, 13 subfractions (F31-43) were collected (Figure 2), and screened for their *in vitro* cytotoxic activity (Table 4).

Of the 13 subfractions (F31-43), only fraction F36 was found to display any marked cytotoxic activity, and did so against all five tested cell lines including the BT474 cell line that appeared insensitive to the parental F26 fraction. However, fraction F36 was not pure enough for structure analysis and so it was further fractionated by silica gel

size exclusion CC, yielding four subfractions (F44-47). Cytotoxicity screening of these four fractions revealed that only fraction F45 was active against all five human cancer-derived cell lines, ranging from a strong activity against the Hep-G2 and Chago I cell lines to a moderate activity against the KATO-III cell line (Table 5). Fraction F46 also showed a cytotoxic activity, but was typically less marked than that for F45 and also was not active against the Hep-G2 cell line. Note, however, that F45 and F46 were less cytotoxic than doxorubicin, a current chemotherapeutic drug, and were cytotoxic towards the normal skin fibroblast cell line CCD-986sk.

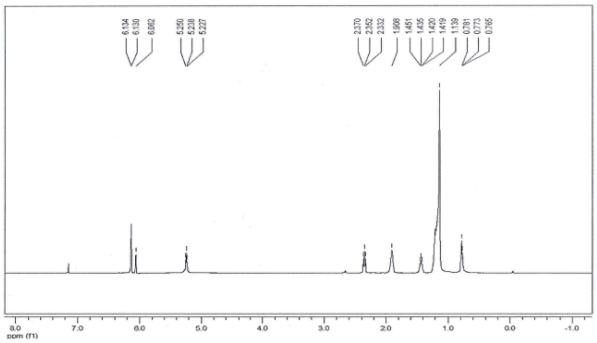

Supplement 1. The ^{1}H NMR spectra of fraction 45

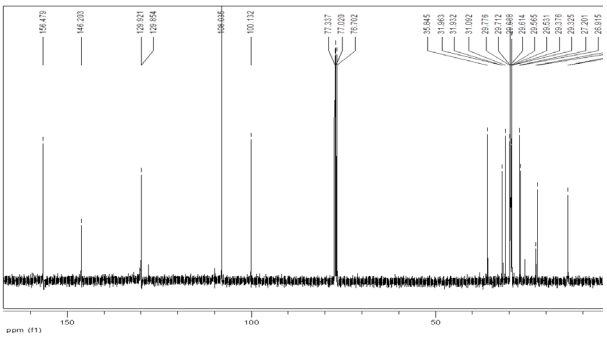

Supplement 2. The ^{13}C NMR spectra of fraction 45

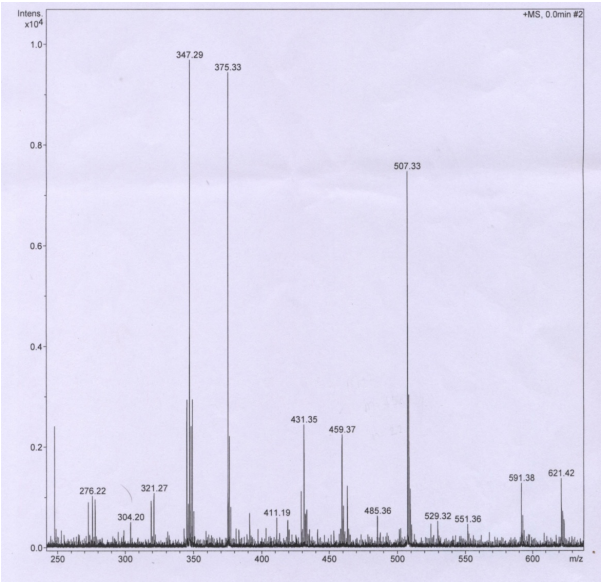

Supplement 3. The mass spectrum data of fraction 45

From the TLC analysis of the four fractions F44-47, only fraction F45 showed an almost clear peak pattern, and so was further analyzed by NMR (Supplements 1 and 2) and MS (supplement 3). Considering the 1H-NMR and 13C-NMR analysis, the main compound in fraction F45 was deduced to be 5-pentadecyl resorcinol (C21H36O2), an isomer structure of cardol (Figure 3).

From the five human cancer derived cell lines, the SW620 colon cancer cell line was selected to screen for the ability of F45 to induce apoptosis (programmed cell death) and /or cell cycle because the morphology of dead cardol-treated SW620 cells has been previously reported (Teerasripreecha et al., 2012). Here, SW620 was treated with F45 at three concentrations (the IC_{20}, IC_{50} and IC_{80}; namely 1.01, 4.51 and 6.84 μg/mL, respectively) for the indicated times and then stained with annexin V and PI and analyzed by flow cytometry. After 24 h incubation, the number of necrotic cells was markedly increased in the F45-treated cells (19.9%) and doxorubicin-treated cells (24.3%) compared to the untreated (3.4%) control cells (Figure 4). After 24-72 h of incubation, a mixture of apoptotic and necrotic cells were seen in the doxorubicin treated cultures, whereas apoptosis and especially early apoptosis was induced at 6 h of incubation and earlier by F45 (Figure 5). Moreover, F45 induced cell cycle arrest of the SW620 cells at the G1 subphase treatment (Figure 6).

Discussion

The CEE of propolis from Trigona incisa harvested in Indonesia was previously reported to have the highest cytotoxic activity against the colon cancer (SW620) cell line (Percentage of survival (PS) 8% at 20 μg/mL) (Kustiawan et al., 2014). Here, we attempted to find the active chemical compound(s) in that propolis using chromatography based fractionation and NMR analysis. An unresolved long chain fatty acid (fraction 21) and cardol isomer (fraction 45) were found to be active cytotoxic compounds against the SW620 cell line (Figure 2).

Many reports have presented the importance of fatty acids in terms of both benefits and dangers. For example, long chain n-3 polyunsaturated fatty acids (PUFA), such as eicosapentaenoic acid and docosahexaenoic acid, can inhibit mammary carcinogenesis or breast cancer efficiently (Liu et al., 2014). The PUFA can be split into the two major classes of n-6 PUFA and n-3 PUFA that can not be endogenously synthesized by humans and so are essential dietary fatty acids (Anderson et al., 2009). In contrast, saturated fatty acids, monounsaturated fatty acids and transfatty acids can all increase the risk of cancer (Saadatian-Elahi et al., 2004). Diet and supplement foods containing high levels of these PUFA could be of interest for anti-cancer effects. In the future, a more complete analysis of the long chain fatty acid in fraction F21 should be completed.

The cytotoxic fraction F46 was found to be impure, but revealed a terpenoid-like pattern while fraction F45 showed a clear 1D-TLC pattern (almost pure) and was deduced to be 5-pentadecyl resorcinol (C21H36O2), an isomer of cardol (Figure 3) (Kubo et al., 1994).

Cardol has been found in many edible plants, such as cashew (Anacardiaceae occidentale), pistachio (Pistacia vera), macadamia (Macademia ternifolia) and mango (Mangifera indica) (Cojocaru et al., 1986), as well, as in inedible parts, such as cashew nut shell liquid (CNSL). In addition to this study showing that cardol was an active compound in Indonesian propolis of T. incisa, it has also been reported from Thai Apis mellifera propolis (Teerasripreecha et al., 2012). With respect to the plants surrounding the apiaries in both countries where the propolis was collected from, it is of interest that both areas were full of mango and cashew nut trees.

Cardol is also of interest in the biotechnology, biopharmacy and biomedicine fields, as an antimicrobial and antitumor agent, molluscicide and prostaglandin synthetase inhibitor (Tocco et al., 2009). It can prevent xanthine oxidase from generating superoxide radicals without inhibiting uric acid formation (Masuoka et al., 2015), and acts as an insecticide and antimicrobial agent though its action on antioxidant enzymes (Trevisan et al., 2006; Lomonaco et al., 2009). The mechanism of action of cardol has been explained by the amphipathic concept of the different head and tail moieties, like polygodial (Fujita et al., 2005). The hydrophilic head portion of cardol binds to the cell membrane surface, while the hydrophobic portion forms a pore that results in the transmembrane transport of other cardol molecules into the cell and subsequent induction of cytotoxicity. Thus, in this scenario, the molecular lipophilicity of cardol seems to be important for its cytotoxicity. However, Kubo et al. (2011) suggested that the balance between the hydrophilic and hydrophobic moieties in cardol was related to their activity. Furthermore, the bactericidal activity of cardol isolated from CNSL was reported to be related to the level of radical oxygen species (Murata et al., 2013), where high doses of cardol induce leakage of K^+ from bacterial cells. In addition, an overdose of cardol might disrupt the native membrane-associated function as it acts as a surfactant.

Here, it was reported that F45 (cardol) can induce cell death by apoptosis at the early period of incubation (≤6 h), but longer exposure (≥24 h) induces necrosis. This observation was consistent with a previous study on SW620 cell morphology following treatment with cardol (Teerasripreecha et al., 2012), and suggests that the treatment time should be of concern. In addition, during the same 24-72 h exposure period, doxorubicin, an anthracycline, induced SW620 cell death by late necrosis. The principal mechanism of action of doxorubicin is known to be via intercalation with DNA to block the progression of topoisomerase-2. This results in the inhibition of DNA replication, and so it has been widely used to treat a wide range of cancers (Pommier et al., 2012).

Cell cycle dysregulation is one of the obvious events in cancer cells. The cell cycle is mediated by the activation of cyclin dependent kinases (CDKs) through binding to cyclins, the specific regulatory subunits (Nigg, 1995). In this present study here, it was found that F45 (cardol) induced cell cycle arrest in the G1 subphase in SW620 cells (Figure 6), suggesting that cardol probably affected either the expression or function of CDKs and/or cyclin.

Cardol has previously been characterized as a cytotoxic agent against several solid tumor cell lines (Kubo et al., 1993). Together with many bioactivities, propolis has increased in value in recent years, especially in countries where the bee industry is widely managed. Propolis may thus become one of the most important bee products and could be an important additive in many products, such as toothpaste, soap and lotions. It has started to become recognized as such in commercial terms. Thus, considerable potential for its further exploitation exists. A new therapeutic agent with a known inhibition mechanism on multiple oncogenic pathways is of paramount importance.

Acknowledgements

We wish to thank the "*Kaltim Cemerlang*" Scholarship of East Kalimantan, Indonesia. In addition, this research was funded by the Ratchadapisek Sompoch Endowment Fund of Chulalongkorn University (RES560530041-FW and Sci-Super 2014-019). We also thank Dr. Robert Butcher for manuscript preparation. The helpful suggestions of anonymous referees and the Editor are acknowledged.

References

Anderson BM, Ma DW (2009). Are all n-3 polyunsaturated fatty acids created equal? *Lipids Health Dis*, **8**, 33

Bankova V, Popova M (2007). Propolis of stingless bees: a promising source of biologically active compounds. *Pharmacogn Rev*, **1**, 88

Boorn K, Khor YY, Sweetman E, et al (2010). Antimicrobial activity of honey from the stingless bee Trigona carbonaria determined by agar diffusion, agar dilution, broth microdilution and time-kill methodology. *J Appl Microbiol*, **108**, 1534-43

Burdock GA (1998). Review of the biological properties and toxicity of bee propolis (propolis). *Food Chem Toxicol*, **36**, 347-63

Cojocaru M, Droby S, Glotter E, et al (1986). 5-(12-Heptadecenyl)-resorcinol, the major component of the antifungal activity in the peel of mango fruit. *Phytochem*, **25**, 1093-5

Donzelli E, Carfì M, Miloso M, et al (2004). Neurotoxicity of platinum compounds: comparison of the effects of cisplatin and oxaliplatin on the human neuroblastoma cell line SH-SY5Y. *J Neurooncol*, **67**, 65-73

Franchin M, da Cunha MG, Denny C, et al (2012). Geopropolis from Melipona scutellaris decreases the mechanical inflammatory hypernociception by inhibiting the production of IL-1β and TNF-α. *J Ethnopharmacol*, **143**, 709-15

Fujita K, Kubo I (2005). Multifunctional action of antifungal polygodial against saccharomyces cerevisiae: involvement of pyrrole formation on cell surface in antifungal action. *Bioorg Med Chem*, **13**, 6742-77

Iwasaki M, Tsugane S (2011). Risk factors for breast cancer: epidemiological evidence from Japanese studies. *Cancer Sci*, **102**, 1607-14

Jeong Y, Cheon J, Kim TO, et al (2014). Conventional cisplatin-based combination chemotherapy is effective in the treatment of metastatic spermatocytic seminoma with extensive rhabdomyosarcomatous transformation. *Cancer Res Treat*, [Epub ahead of print]

Kubo I, Kinst-Hori I, Yokokawa Y (1994). Tyrosinase inhibitors

from Anacardium occidentale fruits. *J Nat Prod*, **57**, 545-52

Kubo I, Nitoda T, Tocoli FE, Green IR (2011). Multifunctional cytotoxic agents from Anacardium occidentale. *Phytother Res*, **25**, 38-45

Kubo I, Ochi M, Vieira PC, Komatsu S (1993). Antitumor agents from the cashew Anacardium occidentale apple juice. *J Agric Food Chem*, **41**, 1012-5

Kustiawan PM, Puthong S, Arung ET, Chanchao C (2014). *In vitro* cytotoxicity of indonesian stingless bee products against human cancer cell lines. *Asian Pac J Trop Biomed*, **4**, 549-56

Liu Y, Bi T, Shen G, et al (2014) Lupeol induces apoptosis and inhibits invasion in gallbladder carcinoma GBC-SD cells by suppression of EGFR/MMP-9 signaling pathway. *Cytotechnology*, [Epub ahead of print]

Liu J, Ma DW (2014). The role of n-3 polyunsaturated fatty acids in the prevention and treatment of breast cancer. *Nutrients*, **6**, 5184-223

Lomonaco D, Santiago GMP, Ferreira YS, et al (2009). Study of technical CNSL and its main components as new green larvicides. *Green Chem*, **11**, 31-3

Massaro CF, Katouli M, Grkovic T, et al (2014). Anti-staphylococcal activity of C-methyl flavanones from propolis of australian stingless bees (tetragonula carbonaria) and fruit resins of corymbia torelliana (Myrtaceae). *Fitoterapia*, **95**, 247-57

Masuoka N, Nihei K, Maeta A, Yamagiwa Y, Kubo I (2015). Inhibitory effects of cardols and related compounds on superoxide anion generation by xanthine oxidase. *Food Chem*, **166**, 270-4

Murata W, Tanaka T, Kubo I, Fujita K (2013). Protective effects of α-tocopherol and ascorbic acid against cardol-induced cell death and reactive oxygen species generation in Staphylococcus aureus. *Planta Med*, **79**, 768-74

Nigg EA (1995). Cyclin-dependent protein kinases: key regulators of the eukaryotic cell cycle. *Bioassays*, **17**, 471-80

Pommier Y, Leo E, Zhang H, Marchand C (2012). DNA topoisomerases and their poisoning by anticancer and antibacterial drugs. *Chem Biol*, **17**, 421-33

Saadatian-Elahi M, Norat T, Goudable J, Riboli E (2004). Biomarkers of dietary fatty acid intake and the risk of breast cancer: a meta-analysis. *Int J Cancer*, **111**, 584-91

Shokoohinia Y, Hosseinzadeh L, Alipour M, Mostafaie A, Mohammadi-Motlagh HR (2014). Comparative evaluation of cytotoxic and apoptogenic effects of several coumarins on human cancer cell lines: osthole induces apoptosis in p53-deficient H1299 cells. *Adv Pharmacol Sci*, **2014**, 847574.

Stetler-Stevenson WG, Kleiner Jr. DE (2001). Molecular biology of cancer: invasion and metastases. In 'Cancer: Principles and Practice of Oncology, 6th ed.', Eds De Vita VT, Hellman S and Rosenberg SA. Lippincott, Williams and Wilkins, Pennsylvania pp 123-36

Teerasripreecha D, Phuwapraisirisan P, Puthong S, et al (2012). *In vitro* antiproliferative / cytotoxic activity on cancer cell lines of a cardanol and a cardol enriched from Thai Apis mellifera propolis. *BMC Complement Altern Med*, **12**, 27

Tocco G, Fais A, Meli G, et al (2009). PEG-immobilization of cardol and soluble polymer-supported synthesis of some cardol-coumarin derivatives: preliminary of their inhibitory activity on mushroom tyrosinase. *Bioorg Med Chem Lett*, **19**, 36-9

Trevisan MTS, Pfundstein B, Haubner R, et al (2006). Characterization of alkyl phenols in cashew (Anacardium occidentale) products and assay of their antioxidant capacity. *Food Chem Toxicol*, **44**, 188-97

Wetherell D, Lawrentschuk N, Gyomber D (2013) Spermatocytic seminoma with sarcoma: an indication for adjuvant chemotherapy in localized disease. *Korean J Urol*, **54**, 884-7

Yaacob NS, Kamal NN, Norazmi MN (2014). Synergistic anticancer effects of a bioactive subfraction of Strobilanthes crispus and tamoxifen on MCF-7 and MDA-MB-231 human breast cancer cell lines. *BMC Complement Altern Med*, **14**, 252